

## Study of Nanostructured Co and Al doped ZnO films

Atikur Rahman<sup>\*</sup>, Chitrashi Mahajan

Department of Metallurgical and Materials Engineering, National Institute of Technology Srinagar, Hazratbal, Kashmir, India

### Article Info

Article history:

Received 2 January 2015

Received in revised form

10 January 2015

Accepted 30 November 2015

Available online 15 December 2015

### Keywords

Doped ZnO Film,

Electroless,

Magnetism,

Dilute Magnetic Semiconductor

### Abstract

Electroless Co( $x = 0.04, 0.03, 0.02$ ) and Al( $y = 0.01, 0.02, 0.03$ ) doped ZnO nanostructured thin films have been deposited on soda lime glass in the present work. The wet deposited films are dried in air and subsequently annealed at 500°C for 2 hr in a muffle furnace in air environment. The film deposited samples are characterized by SEM, XRD, Superconducting quantum interference device (SQUID) magnetometer and UV visible spectrophotometer. Microstructure of the Co and Al doped ZnO film is strongly affected by different doping concentration into ZnO matrix. X-ray diffraction analysis confirms the absence of metallic Co or Al clusters or any other phase different from wurtzite type ZnO. The field dependence of magnetization (M-H) curve of different concentration of Co and Al doped ZnO films measured at room temperature exhibits the clear ferromagnetism with saturation magnetization (Ms) and coercive field (Hc) of the order of 3.843 to 4.813  $10^{-3}$ (emu) and 400.389 to 436.769(Oe) respectively. It is found that ferromagnetism increased correspondingly with Co concentration. The relevant ferromagnetism mechanisms at room temperature in Co and Al doped ZnO films are discussed.

## 1. Introduction

There has been great interest in growth and characterization of dilute magnetic semiconductors for their potential technological application to transparent spintronics devices such as spin solar cells, spin light emitting diodes, optical isolators and ultra fast optical switches. Dilute magnetic semiconductors are produced by introducing small fraction of transition metals into non-magnetic host semiconductors e.g. III-V and II-VI compounds [1]. Wide band gap semiconductors such as Gd doped ZnO have been identified as promising dilute magnetic semiconductor materials as they exhibit ferromagnetism at room temperature and are optically transparent to visible light [2]. Opto and magneto electronics application point of view ZnO is attractive because of high exciton binding energy = 60 meV and band gap = 3.3 eV [3]. It is resistive to high energy radiation, environmentally friendly, easily available and economical. Heavy electron doping is possible in ZnO by using appropriate donor dopant of group III elements like Al, Ga, In. Dilute magnetic semiconductor materials point of view, this feature can be promising for strong ferromagnetic exchange coupling between localized spins due to carrier induced ferromagnetism such as Ruderman-Kittel-Kasuya-Yosida interaction and double exchange interaction [4]. In case of Co and Al codoped ZnO system, extra carriers provided by Al interact with Co atoms thereby introducing permanent dipole moments aligned in one direction. Al acts as donor dopant by providing a free electron for conduction in the dilute magnetic semiconductor system. It also provides optical transparent films in the visible region for magneto-optical devices.

Al doped ZnO films have been investigated by many research [5, 6] because they have potential applications in a variety of opto-electronic devices such as solar cells, flat

panel displays and transparent heat mirrors. ZnO films doped with magnetic metals, for example, Co, Ni, Fe, have been studied as diluted magnetic semiconductors [7, 8]. Tominaka et al [9] reported the sputter deposited Co-doped ZnO: Al films and then heated them in air from room temperature to 673 K. They found that the conductivity of the films is stable until 573 K. Minami et al [10] prepared Co-doped ZnO: Al films by DC magnetron sputtering with a mixture target of ZnO, Al<sub>2</sub>O<sub>3</sub> and CoO (or CoCl<sub>2</sub>). They found that the Co-doped ZnO:Al films exhibited better chemical stability without a significant alteration of the original electrical and optical properties after HCl and KOH etched. Most of the researchers [6, 10] reported the development of Co and Al doped ZnO film by RF-magnetron sputtering process. Very limited literature is available on magnetic metals and Al doped ZnO thin films by electroless process. Since, the deposition of thin films by magnetron / pulse laser process (PVD process) is complex process as it requires high vacuum and costly target materials. Also, size of the samples deposited is limited.

In the present research work, Co and Al doped ZnO films with different mole fraction are developed by electroless deposition process and its advantages are given below:

- The process is simple, cheap, easy to handle and no sophisticated elements or instruments are required [11, 12].
- Good adherence between films and substrate can be obtained. Dopant addition can be easily controlled by altering composition of inorganic precursors. Also, there is flexibility of size and shape of the sample for deposition of the film by electroless.

### Draw backs of electroless process:

Chemical bath cannot be re-used. Therefore, only required capacity of the chemical bath is prepared at a time, while in magnetron sputtering process, target can be re-used provided a central hole is not formed in the target.

### Corresponding Author,

E-mail address: atikurrhmn@gmail.com

All rights reserved: <http://www.ijari.org>

The aim of the present research work is to study the effects of doping on structural, optical and magnetic properties of  $\text{Co}(x = 0.04, 0.03, 0.02)$  and  $\text{Al}(y = 0.01, 0.02, 0.03)$  doped ZnO nanostructured electroless thin films. Electroless film process has an advantage of low cost fabrication in which the mole fractions of ternary and quaternary compounds can be controlled accurately.

## 2. Experimental Procedure

### 2.1 Preparation of Plating Bath

The electroless bath solution is prepared using Zinc-Acetate-2-Hydrate [ $\text{Zn}(\text{O}_2\text{CCH}_3)_2 \cdot 2(\text{H}_2\text{O})$ ] (Sigma Aldrich, purity 99.99%), Cobalt Sulphate [ $\text{CoSO}_4 \cdot 7(\text{H}_2\text{O})$ ] (Sigma Aldrich, purity 99.99%), Aluminum-Nitrate-9-Hydrate [ $\text{Al}(\text{NO}_3)_3 \cdot 9(\text{H}_2\text{O})$ ] (Sigma Aldrich, purity 99.99%) and Diethanolamine (Analytical Grade).  $\text{Co}(x = 0.04, 0.03, 0.02)$  and  $\text{Al}(y = 0.01, 0.02, 0.03)$  doped ZnO thin films have been prepared in the laboratory using electroless process. Mole fraction  $\text{Co}(x = 0.04, 0.03, 0.02)$  and  $\text{Al}(y = 0.01, 0.02, 0.03)$  of the constituent element in the films has been controlled by adjusting the Co and Al to Zn weight ratio. The above chemicals are used without any further purification. Initially, appropriate amount of Zinc Acetate and Diethanolamine are dissolved in distilled water and was stirred at  $60^\circ\text{C}$  for 2 h. Then, Cobalt- Sulphate- 7-Hydrate and Aluminum-Nitrate-9-Hydrate with different mole fraction ( $x = 0.00$  to  $0.04$  with step of  $0.01$  and  $y = 0.00$  to  $0.03$  with step of  $0.01$ ) are added to it and the final solution is stirred for additional 2 hours, which served as bath solution after cooling to ambient temperature.

### 2.2 Plating, Drying and Annealing the Sample

Soda-lime glass substrate (dimension:  $25 \times 25 \times 1.33 \text{ mm}^3$ ) is used and it is cleaned in acetone and distilled water. Finally, clean glass substrate is dipped into the electroless bath at  $90^\circ\text{C}$  temperature for 2 hr. After 2 hr dipping of the sample, the wet deposited samples are dried in air at room temperature. Samples are kept in the plating position to avoid draining and blending of the just deposited wet-films, which could lead to irregularities in the layer thickness and to surface inhomogeneties. The deposited films are heat treated in a muffle furnace for 2 hr in air at  $500^\circ\text{C}$  temperatures. A series of samples are prepared with different mole fraction of  $\text{Co}(x = 0.00, 0.04, 0.03, 0.02)$  and  $\text{Al}(y = 0.00, 0.01, 0.02, 0.03)$ . Standard conditions for synthesizing of different mole fraction of Co and Al doped ZnO films are shown in **Table 1**. The structural characteristics are examined using X-ray diffraction (XRD), scanning electron microscope (SEM). The optical properties of the samples are analyzed by spectrophotometer in the spectral range 300-600 nm. Magnetic measurements are taken with superconducting quantum interference device (SQUID) magnetometer (QD MPMSXL). Crystal structure of Co and Al doped ZnO films are determined by powder X-ray diffraction. XRD data of the samples are taken using a Bruker AXS D8 advance diffractometer with  $\text{CuK}_\alpha$  target ( $\lambda = 1.54052 \text{ \AA}$ ) radiation over the range  $2\theta = 10-80^\circ$  with a step of  $0.01^\circ$  at room temperature. The surface morphology is determined by scanning electron microscope (SEM-LEO 534).

**Table: 1.** Standard conditions for synthesis of  $\text{Co}(x = 0.00, 0.04, 0.03, 0.02)$  and  $\text{Al}(y = 0.00, 0.01, 0.02, 0.03)$  doped ZnO nanostructured films

Mole Fraction Co(x)	Zinc-Acetate- -2-Hydrate Al(y)	Aluminum-Nitrate- - 9-Hydrate	Diethanolamine	Cobalt Sulphate
Synthesis precursors Molarity (M)				
0.00	0.00	0.5	0.000	0.5
0.02	0.03	0.5	0.010	0.5
0.03	0.02	0.5	0.015	0.5
0.04	0.01	0.5	0.020	0.5

## 3. Results and Discussion

### 3.1 X-Ray Diffraction (XRD)-Structural Studies

Fig.1 (a) Shows the X-ray diffraction patterns of  $\text{Co}(x = 0.000, 0.04, 0.03, 0.02)$  and  $\text{Al}(y = 0.000, 0.01, 0.02, 0.03)$  doped ZnO nanostructured films. XRD results indicated that all the samples showed hexagonal wurtzite structures without any characteristic peaks of impurities. The major peaks are identified as (100), (002), (101), (102), (110), (103), (200), (112), and (201) planes of reflections for wurtzite structure of ZnO according to PCPDFWIN CAS Number: PDF#800075. The (101) peak shows the highest intensity in all cases, implying that all the samples have a hexagonal crystal structure with a preferred orientation.

There are no detectable diffraction peaks for Co and Al metal clusters, Co or Al oxide secondary phases or other impurity phases within the sensitivity of our XRD measurements, implying that Co ions and Al ions are incorporated into the interstitial site of ZnO lattice sites. In addition, compared with un-doped ZnO nanostructured film, increasing Co and Al doping concentration caused a shift in diffraction peak position of the Co and Al doped ZnO nanostructured films. The ionic radii of  $\text{Zn}^{+2}$ ,  $\text{Co}^{+2}$  and  $\text{Al}^{+3}$  are  $0.72 \text{ \AA}$ ,  $0.58 \text{ \AA}$  and  $0.57 \text{ \AA}$  respectively [13]. These seem to be an easy 'fitting in' of Co and Al, which helps to improve the preferred growth along (101). For a better comparability, Fig. 1(b) shows the X-ray diffraction patterns of un-doped ZnO and different concentration of  $\text{Co}(x = 0.00,$

0.04, 0.03, 0.02) and Al (y = 0.00, 0.01, 0.02, 0.03) doped ZnO nanostructured films, only in the detection angle range of the preferred orientations. It can be seen that the peaks are shifted towards lower angles as compared to un-doped ZnO and intensity of the peaks are also decreasing by increasing the doping concentration. It confirms the easy fit of Co ions and Al ions into ZnO lattice. The average crystal size of the samples is determined from the broadening of the diffraction peaks (100), (002) and (101) plane using Debye–Scherrer’s formula [14],

$$D = \frac{k\lambda}{B \cos \theta} \quad (1)$$

Where ‘D’ is the average size of crystallite, ‘B’ is the broadening of the diffraction line measured at half maximum intensity, k is constant (k=1 is used in the present work [14]),  $\lambda$  is the wavelength of the X-ray radiation (1.54052 Å, CuK $\alpha$ ) and  $\theta$  is the Bragg angle. Instrumental broadening has been accounted for the calculation of grain size, and its value of 0.1(for standard Si sample) has been subtracted from the full-width half maximum (FWHM) value, from B value. Moreover, the observed slight shift of the major diffraction peaks towards a lower diffraction angle with increase in Co and Al concentrations suggested that Co<sup>+2</sup> and Al<sup>+3</sup> ions would uniformly occupy interstitial sites in ZnO lattice. Table 2 shows the  $2\theta$  and full width at half maximum (FWHM) values, cell parameters ‘a’ and ‘c’, d value and average crystal size (D) and lattice strain for the different Co and Al concentrations, where lattice strain are calculated using the formula [15],

$$\text{Lattice strain } (\varepsilon) = \frac{BCos\theta}{4} \quad (2)$$

Therefore, the increase in lattice parameters and a small shift of main peaks of ZnO into lower angles reveals that the interstitial incorporation of Co ions and Al ions into ZnO lattice [16, 17]. The small change in diffraction peaks and the broadening are due to the increase of lattice strain.

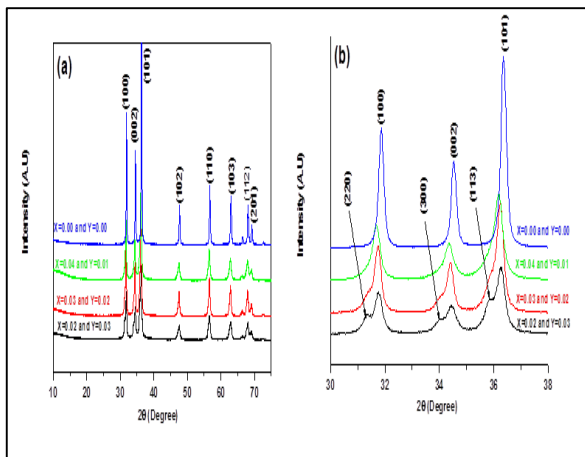


**Fig: 1(a).** XRD patterns of un doped ZnO and Co(x = 0.00, 0.04, 0.03, 0.02) and Al(y = 0.00, 0.01, 0.02, 0.03) doped ZnO nanostructured films and (b) XRD patterns of un doped ZnO and Co(x = 0.00, 0.04, 0.03, 0.02) and Al(y = 0.00, 0.01, 0.02, 0.03) doped ZnO nanostructured films, only in the detection angle range of the preferred orientations for better comparability.

*Table 2 The  $2\theta$  and full width half maximum (FWHM) values, cell parameters ‘a’ and ‘c’, d value, average crystal size(D) and lattice strain( $\varepsilon$ ) of Co and Al doped nanostructured films*

Mole Fraction	$2\theta$ Value (deg)	FWHM (deg)	Cell parameter (Å)		d value (Å)	Average Crystal Size D(nm)	Lattice Strain ( $\varepsilon$ )( $10^{-5}$ )	
			a	c				
Co(x)	Al(y)							
0.00	0.00	36.35	0.16	3.4933	4.2802	2.4705	77.4	0.562
0.02	0.03	36.16	0.23	3.4995	4.2879	2.4749	24.2	0.810
0.03	0.02	36.26	0.24	3.4944	4.2817	2.4713	27.6	0.844
0.04	0.01	36.24	0.29	3.4981	4.2862	2.4739	22.9	1.020

### 3.2 SEM Microstructure of the Films

Fig. 2(a-d) show the surface SEM microstructure of undoped and Co(x = 0.00, 0.04, 0.03, 0.02) and Al(y = 0.00, 0.01, 0.02, 0.03) doped ZnO nanostructured thin films. Fig.2 (a) represents the micrograph of undoped ZnO film and has large rod type grains with voids. Fig.2 (b-d) shows the surface morphology of Co(x = 0.04, 0.03, 0.02) and Al(y = 0.01, 0.02, 0.03) doped ZnO nanostructured thin films. Fig.2 (b) shows the microstructure of Co(x = 0.02) and Al(y = 0.03) doped ZnO nanostructured thin and has small thin rod type grains. According to the micrographs, the film morphology shows a dependence on the doping concentration. In general, the grain shape and size change with the doping concentrations, although a meticulous observation, allows us to see as the large spherical shape grains present in Co(x = 0.03) and Al(y = 0.02) doped ZnO nanostructured thin film (Fig.2. (c)). Co(x = 0.04) and Al(y = 0.01) doped ZnO nanostructured thin film (Fig.2 (d)) shows homogeneous and dense surfaces covered by small-size grains and free from voids. From SEM analysis it has been observed that Co and Al as do pant into ZnO matrix play a great role in tuning of microstructure. Co<sup>+2</sup> ions and Al<sup>+3</sup> ions occupy the interstitial position into ZnO lattice and retard the grain growth of ZnO film. Due to this reason, Co(x = 0.02) and Al(y = 0.03) doped ZnO film has small thin rod type grain as compared to undoped ZnO film (Fig.2 (a)). When we increased the concentration of Co(x = 0.03) and reduced the concentration of Al(y = 0.02) into doped ZnO film, thin rod type grains transformed into spherical shape grains (Fig.2. (c)). Further, we increased the concentration of Co(x = 0.04) and reduced the concentration of Al(y = 0.01) into doped ZnO film, small spherical shape grains with dense microstructure is found (Fig.2. (d))

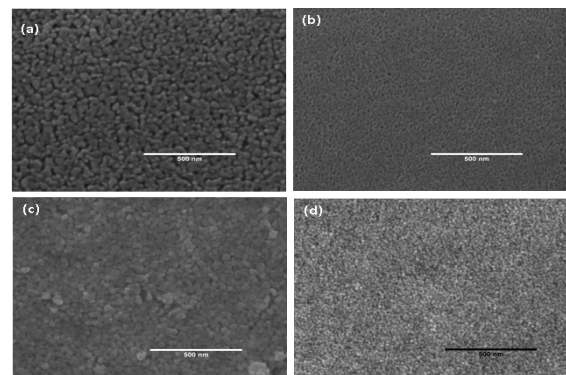


**Fig: 2(a-d)** SEM surface morphology of undoped ZnO and Co(x = 0.00, 0.04, 0.03, 0.02) and Al(y = 0.00, 0.01, 0.02, 0.03) doped ZnO nanostructured films, (a) undoped ZnO film, (b) Co(x = 0.02) and Al(y = 0.03) doped ZnO film, (c) Co(x = 0.03) and Al(y = 0.02) doped ZnO film, (d) Co(x = 0.04) and Al(y = 0.01) doped ZnO film

### 3.3 Photoluminescence Studies

The photoluminescence spectra have been carried out between the wavelength ranges from 300 to 600 nm under the excitation of Xenon lamp laser with 325 nm line using a fluorescence spectrophotometer (F-2500) at room temperature. The photoluminescence emission intensity of the undoped ZnO and different mole fraction of Co(x = 0.04, 0.03, 0.02) and Al(y = 0.01, 0.02, 0.03) doped ZnO films are shown in Fig. 3. It can be seen that the emission intensity of photo luminescent of different mole fraction of Co(x = 0.04, 0.03, 0.02) and Al(y = 0.01, 0.02, 0.03) doped ZnO films have lower value as compared to undoped ZnO film. Among them Co(x = 0.04) and Al(y = 0.01) doped ZnO film has lowest value of photoluminescence intensity. The photoluminescence emission intensity is related to the recombination of excited electrons and holes, and thus, the lower emission intensity is inductive of a decrease in recombination rate [18, 19]. Fig. 3 revealed that the Co(x = 0.04) and Al(y = 0.01) doped ZnO film has minimum recombination of electron-hole pairs. The process of recombination of carriers is opposite to that of the generation of carriers. In this process, excited electrons fall back from the conduction band to the valence band, reoccupying an empty energy state (a hole) in the valence band, thus electron-hole pairs get destroyed. The recombination of generated carriers is not desirable on the surface of dilute magnetic semiconductors and should be avoided as much as possible.

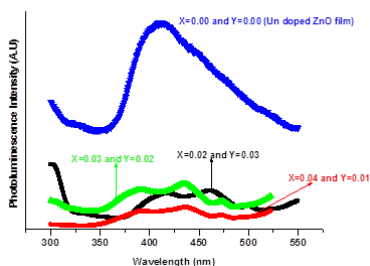


**Fig: 3.** Photoluminescence emission spectra of undoped ZnO film and Co(x = 0.04, 0.03, 0.02) and Al(y = 0.01, 0.02, 0.03) doped ZnO nanostructured films for better comparison of intensity of photoluminescence.

### 3.4 Magnetic characterization

The magnetic properties of the Co(x = 0.00, 0.04, 0.03, 0.02) and Al(y = 0.00, 0.01, 0.02, 0.03) doped ZnO nanostructured films are investigated at room temperature with superconducting quantum interference device (SQUID) magnetometer (QD MPMSXL). We observed distinct ferromagnetic behavior in the doped samples only, no trace of ferromagnetism is observed in the undoped ZnO sample that is tested under similar conditions using the SQUID. Fig. 4(a) shows the magnetic hysteresis (M-H) loop for

Co(x = 0.03) and Al(y = 0.02) doped ZnO nanostructured film. The saturation magnetization ( $M_s$ ), coercive field ( $H_c$ ) and remanent magnetization ( $M_r$ ) of the sample is  $3.843 \times 10^{-3}$  (emu), 436.769(Oe) and  $2.799 \times 10^{-3}$  (emu) respectively, where as Fig. 4(b) shows the magnetic hysteresis (M-H) loop for Co(x = 0.04) and Al(y = 0.01) doped ZnO nanostructured film. The saturation magnetization ( $M_s$ ), coercive field ( $H_c$ ) and remanent magnetization ( $M_r$ ) of the sample is  $4.831 \times 10^{-3}$  (emu), 400.389(Oe) and  $3.132 \times 10^{-3}$  (emu). Fig. 4(c) shows the magnetization curve for Co(x = 0.02) and Al(y = 0.03) doped ZnO nanostructured film, which exhibits ferromagnetic behavior with a small coercive field and remanent magnetization with low magnetized narrow hysteresis loop. No saturation magnetization is reached in this sample with applied fields  $H = 10000$  (Oe). The change in  $M_s$  and  $H_c$  for different concentration of Co and Al doped ZnO nanostructured films are compared (Fig.4 (a-c)). It is found that  $M_s$  value is higher for Co(x = 0.04) and Al(y = 0.01) doped ZnO film and the  $M_s$  increases with increasing the doping concentration. Higher  $M_s$  in Co(x = 0.04) and Al(y = 0.01) doped ZnO film is likely to be caused by enhanced doping and higher ferromagnetism ordering in ZnO. Increased ferromagnetism might be possible with the combined features of Co and Al doping in ZnO and extended defects may be responsible. Doping of metals (Co and Al) essentially plays the key role to the observed ferromagnetism. It may be noted that high  $M_s$  value at room temperature in the Co(x = 0.04) and Al(y = 0.01) doped ZnO film observed in this study. It is likely that due to large density of point defects as well as extended defects such as dislocations associated with the strain in the ZnO lattice, magnetic interactions mediated by the interaction of doping and defects is enhanced in the doped ZnO films. It is expected that samples with higher concentration of defects/strain would show higher magnetization. From XRD analysis it has been confirmed that Co(x = 0.04) and Al(y = 0.01) doped ZnO film has highest lattice strain (Table-2).

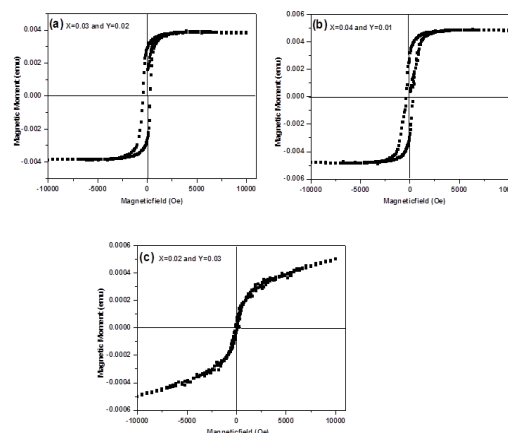


**Fig: 4(a-c)** room temperature field vs magnetization (M-H) loop showing hysteresis of the Co(x = 0.04, 0.03, 0.02) and Al(y = 0.01, 0.02, 0.03) doped ZnO nanostructured films, (a) Co(x = 0.03) and Al(y = 0.02) doped ZnO film, (b) Co(x = 0.04) and Al(y = 0.01) doped ZnO film, (c) Co(x = 0.02) and Al(y = 0.03) doped ZnO.

#### 4. Conclusions

Co(x = 0.00, 0.04, 0.03, 0.02) and Al(y = 0.00, 0.01, 0.02, 0.03) doped ZnO nanostructured thin films have been synthesized by electroless process. XRD analysis confirmed the hexagonal wurtzite structure without any impurities. The increase of lattice constants, the slight shift of XRD peaks towards a lower angle and the reduction in average crystalline size indicated that Co and Al have really doped into the ZnO lattice. The mechanism for the ferromagnetism at room temperature in Co and Al doped ZnO nanostructured films are possible of the dopant ions. Co(x = 0.04) and Al(y = 0.01) doped ZnO film shows higher  $M_s$  value due to smaller grains size and large amount of lattice strain. It may be highlighted that dense, uniform and small grain size (22.9 nm) of Co(x = 0.04) and Al(y = 0.01) doped

#### References

- [1] H. Ohno, Making Nonmagnetic Semiconductors Ferromagnetic, *Science*, 14, 1998, 951- 956
- [2] S. Shanthi, N. Muthukumarasamy, S. Agilan, R. Balasundaraprabhu, Studies on Gd doped ZnO nanocrystalline thin films, *Materials Research Innovations*
- [3] J. Fan, P. Poosimma, R. Freer, Phase development in ZnO varistors, *Advances in Applied Ceramics*
- [4] D. Hu, Y. J. Liu, H. S. Li, X. Y. Cai, X. L. Yan, Y. D. Wang, Effect of nickel doping on structural, morphological and optical properties of sol-gel spin coated ZnO films, *Materials Technology*, 27, 2012, 243 – 250
- [5] P. J. Cao, S. Han, W. J. Liu, F. Jia, Y. X. Zeng, D. L. Zhu, Y. M. Lu, Effect of oxygen flowrate on optical and electrical properties in Al doped ZnO thin films, *Materials Technology*, 29, 2014, 336 – 340
- [6] S. Yu, Z. Wei, X. X. Dong, Y. Wang, Study of aluminium doped zinc oxide nanofilms deposited by rf magnetron sputtering, *Materials Research Innovations*, 18, 2014, S5-69 - S5-72,
- [7] H. I. Saleh, E. M. El-Meliegy: Nickel or cobalt doped zinc oxide varistors, *British Ceramic Transactions*, 103, 2004, 268 – 272
- [8] D. Hu, Y. J. Liu, H. S. Li, X. Y. Cai, X. L. Yan, Y. D. Wang, Effect of nickel doping on structural, morphological and optical properties of sol-gel spin coated ZnO films, *Materials Technology*, 27, 2012, 243 – 250
- [9] K. Tominaga, T. Takao, A. Fukushima, T. Moriga, I. Makabayashi, Amorphous ZnO-In<sub>2</sub>O<sub>3</sub> transparent conductive films by simultaneous sputtering method of ZnO and In<sub>2</sub>O<sub>3</sub> targets, *Vacuum*, 66, 2002, 505-509
- [10] T. Minami, S. Suzuki, T. Miyata, Transparent conducting impurity-co-doped ZnO: Al thin films

ZnO film can be obtained by low cost electroless process and have optimum combination of optical and magnetic properties. It can be considered to be important steps for the development of semiconductor devices that can retain good ferromagnetism properties at room temperature for the commercial or mobile devices.

#### Acknowledgment

One of the authors, Dr. Atikur Rahman would like to thank Prof.(Dr.) Rajat Gupta, DIRECTOR, NATIONAL INSTITUTE OF TECHNOLOGY SRINAGAR HAZRATBAL, KASHMIR-190006, INDIA for their financial support to this work (Order No. 85 of 2013, Dated:11-07-2013).

- prepared by magnetron sputtering, *Thin Solid Films*, 53-58, 2001, 398–399
- [11] L. L. Wang, H. J. Chen, Z. L. Chen, Study on post-treatments for electroless Ni-P coating, *Surf Eng.*, 27(1), 2011, 57-60
- [12] K. N. Srinivasan, T. Selvaganapathy, R. Meenakshi, S. John, Electroless deposition of nickel-cobalt-phosphorus nanoalloy, *Surf Eng.* 27(1), 65-70, 2011
- [13] M. S. Tokumoto, A. Smith, C. V. Santilli, S.H. Pulcinelli, E. Elkaim, V. Briois, Effect of In concentration in the starting solution on the structural and electrical properties of ZnO films prepared by the pyrosol process at 450°C, *J Non-Cryst Solids*, 273, 2002, 302-306
- [14] D. Zou, D. Yan, L. Xiao, Y. Dong, Characterization of nanostructured TiN coatings fabricated by pulse laser, *Surf. Coat. Technol.*, 202, 1928-1934
- [15] P. P. Hankare, P.A. Chate, D. J. Sathe, P.A. Chavan, V. M. Bhuse, Effect of thermal annealing on properties of zinc selenide thin films deposited by chemical bath deposition, *J Mater Sci –Mater Electron.* 20, 2009, 374-379
- [16] X. h. Sun, R.Y. Cao, Y. Wu, Y. Liu, X. Zhang, Ethanol thermal synthesis and antibacterial properties of Ag modified ZnO nanorods, *Materials Technology*, 2014, 105-111
- [17] B. G. Mishra, G. R Rao, Promoting effect of ceria on the physicochemical and catalytic properties of CeO<sub>2</sub>-ZnO composite oxide catalysts, *J. Mol. Catal. A Chem.*, 243, 204-213, 2006
- [18] R. C. Wang, H.Y. Lin, Hydrothermal synthesis and characterization of ZnO films with different nanostructures, *Mater Chem Phys.* 125, 263-266, 2001
- [19] X. T. Yin, W. X. Que, Y. L. Liao, J. Zhang, F. Y. Shen, Ag-ZnO composite nanocrystals: synthesis, characterisation and photocatalytic properties, *Materials Research Innovations*, 16(3), 213-218, 2012